Fast Uncertainty Quantification of Electromechanical Oscillation Frequency on Varying Generator Damping

Yongli Zhu and Chanan Singh

Abstract—This letter develops a fast analytical method for uncertainty quantification of electromechanical oscillation frequency due to varying generator dampings. By employing the techniques of matrix determinant reduction, two types of uncertainty analysis are investigated to quantify the impact of the generator damping on electromechanical oscillation frequency, i.e., interval analysis and probabilistic analysis. The proposed analytical frequency estimation formula is verified against conventional methods on two transmission system models. Then, Monte Carlo experiments and interval analysis are respectively conducted to verify the established lower/upper bound formulae and probability distribution formulae. Results demonstrate the accuracy and speed of the proposed method.

Index Terms—Electromechanical oscillation, interval analysis, Monte Carlo simulation, quadratic eigenvalue problem, uncertainty quantification.

I. INTRODUCTION

POWER system low-frequency oscillation, also known as electromechanical oscillation, is a common issue in large-scale transmission power systems. Fast identification of the electromechanical oscillation mode (in short, "mode") is an important step in system online monitoring. The oscillation frequency of each mode is typically distinct from each other in a stable power system [1], i.e., one kind of signature of each mode. Thus, the analysis of the mode oscillation frequencies is the focus of this letter. One research concern is the assessment of parameter uncertainties on electromechanical oscillation frequencies, e.g., when the generator damping coefficient D is varying.

The generator damping coefficient is a critical parameter. It can represent the aggregated damping effects of the frequency-dependent load [2] or renewables-based damping controllers [3], [4]. Unlike the generator inertia M with the unit s that can be theoretically derived from the generator's physical parameters (e.g., the moment of inertia J with the

unit $kg \cdot m^2$), the generator damping coefficient is typically assumed or estimated. It should be mentioned that other factors can also influence the oscillation frequencies, e.g., network topology [5]. However, systematic study regarding the uncertainty quantification (UQ) of generator damping on electromechanical oscillation frequency is less reported. Therefore, this letter tries to fill that research gap.

Existing methods for power system related UQ include Gram-Charlier series [6], Cornish-fisher expansion [7], maximum entropy method [8], etc. Unlike those methods that mainly depend on complicated symbolic series expansion and a heavy load of numerical computation, the proposed method in this letter is based on concise analytical formulae derived from the system's mathematical model. Therefore, it involves no effort of symbolic series expansion and requires less numerical computation. Merits of the proposed method are:

1) Faster calculation speed due to the usage of analytical formulae. Thus, it can assist system operators in quickly identifying abnormal oscillation modes from the oscillation frequency results obtained by field measurements.

2) No need for (post-disturbance) time-series of voltage or frequency signals. Thus, it is less affected by measurement noise or data package loss.

Note that the proposed method does not aim to replace other measurement-based or probabilistic small-signal analysis methods but to provide a theoretical baseline for system operators in a quicker manner.

The rest of this letter is organized as follows. In Section II, this letter derives a concise analytical estimation formula for oscillation frequencies by transforming the original standard eigenvalue problem (SEP) into a quadratic eigenvalue problem (QEP) [9], where the matrix dimension is reduced to half. The transformed problem does not need initial guesses as required by Newton-type methods. In Section III, the UQ is presented. Sections IV and V conduct verification experiments on the IEEE 9-bus and WECC 179-bus systems. Conclusions and future work are presented in Section VI.

II. ANALYTICAL ESTIMATION OF OSCILLATION FREQUENCY

A. Small-signal Model of Multi-machine System

An n-generator power system can be reduced to a network with only generator buses [1], as illustrated in Fig. 1.
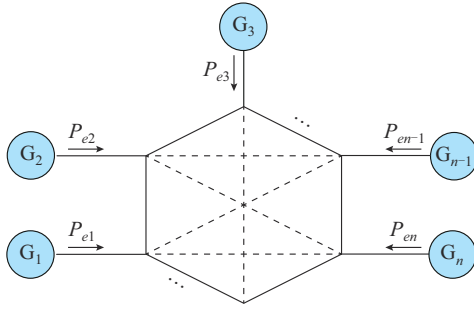
Fig. 1.   Reduced network topology for an n-generator power system.

The electromechanical oscillation frequencies are mainly associated with the generator swing equations [1], [2] and are relatively less affected by higher-order nonlinearities. Thus, the classical, i.e., 2nd-order, model [2] is adopted for each generator in analytical formula derivation. The effectiveness of this handling will be validated in case studies. Then, by linearizing the system differential-algebraic equations (DAEs) around the given equilibrium point, the small-signal model is given as:

$$
\left\{
\begin{aligned}
&\begin{bmatrix} \Delta \dot{\boldsymbol{\delta}} \\ \Delta \dot{\boldsymbol{\omega}} \end{bmatrix} = \begin{bmatrix} \boldsymbol{O} & \Omega_0 \boldsymbol{I} \\ -\boldsymbol{M}^{-1}\boldsymbol{J} & -\boldsymbol{M}^{-1}\boldsymbol{D} \end{bmatrix} \begin{bmatrix} \Delta \boldsymbol{\delta} \\ \Delta \boldsymbol{\omega} \end{bmatrix} \overset{\text{def}}{=\!=} A \begin{bmatrix} \Delta \boldsymbol{\delta} \\ \Delta \boldsymbol{\omega} \end{bmatrix} \\
&\boldsymbol{M} = \text{diag}(M_1, M_2, ..., M_n) \\
&\boldsymbol{D} = \text{diag}(D_1, D_2, ..., D_n) \\
&\boldsymbol{J} = [J_{ij}] \\
&\boldsymbol{O} = [0]_{n \times n} \\
&\Delta \boldsymbol{\delta} = [\Delta \delta_i]_{n \times 1} \\
&\Delta \boldsymbol{\omega} = [\Delta \omega_i]_{n \times 1} \\
&\Omega_0 = 2\pi f_0 \\
&J_{ij} = \sum_{j \neq i}^{n} P_{ij,\max} \sin(\alpha_{ij} - \delta_{ij0}) \quad j = i, P_{ij,\max} = E_i E_j \left| Y_{ij} \right| \\
&J_{ij} = -P_{ij,\max} \sin(\alpha_{ij} - \delta_{ij0}) \quad j \neq i, P_{ij,\max} = E_i E_j \left| Y_{ij} \right|
\end{aligned}
\right.
\tag{1}
$$

where δ_i, ω_i, P_{ei}, E_i, M_i, and D_i $(i = 1, 2, ..., n)$ are the rotor angle, speed, electromagnetic power, internal voltage, inertia, and damping coefficients of the ith generator, respectively; f_0 is the synchronous frequency, e.g., 60 Hz; $\boldsymbol{I}$ is the $n \times n$ identity matrix; $Y_{ij} = G_{ij} + j B_{ij} = \left| Y_{ij} \right| \angle \alpha_{ij}$ is the element of the reduced nodal admittance matrix; $\delta_{ij0} = \delta_{i0} - \delta_{j0}$ is the steady-state rotor angle difference between the ith and the jth generators; and $\boldsymbol{J}$ is the $n \times n$ power-flow Jacobian matrix, which is nearly symmetric for a transmission network due to the small r/x ratios of transmission lines.

B. Analytical Estimation of Eigenvalues

The characteristic equation of the above system matrix is:

$$
\det(\lambda \boldsymbol{I} - A) = \det(\lambda \boldsymbol{I}^{\text{T}} - A^{\text{T}}) = \det \begin{pmatrix} \lambda \boldsymbol{I} & \boldsymbol{J}^{\text{T}} \boldsymbol{M}^{-1} \\ -\Omega_0 \boldsymbol{I} & \lambda \boldsymbol{I} + \boldsymbol{M}^{-1}\boldsymbol{D} \end{pmatrix} = 0
\tag{2}
$$

In (2), the first equality holds since $\det(\boldsymbol{X}^{\text{T}}) = \det(\boldsymbol{X})$ holds for any square matrix $\boldsymbol{X}$. Then, Theorem 3 from [10] is as follows.

Theorem: the identity $\det(\boldsymbol{E}) = \det(\boldsymbol{AD} - \boldsymbol{BC})$ holds for a 2-by-2 block matrix $\boldsymbol{E} = \begin{bmatrix} \boldsymbol{A} & \boldsymbol{B} \\ \boldsymbol{C} & \boldsymbol{D} \end{bmatrix}$, if $\boldsymbol{CD} = \boldsymbol{DC}$.

It is clear that the above theorem condition holds for the bottom two block matrices of (2). Thus, it leads to:

$$
\begin{aligned}
&\det(\lambda \boldsymbol{I}(\lambda \boldsymbol{I} + \boldsymbol{M}^{-1}\boldsymbol{D}) - (\boldsymbol{J}^{\text{T}} \boldsymbol{M}^{-1})(-\Omega_0 \boldsymbol{I})) = 0 \Leftrightarrow \\
&\quad \det(\lambda^2 \boldsymbol{I} + \lambda \boldsymbol{M}^{-1}\boldsymbol{D} + \Omega_0 (\boldsymbol{J}^{\text{T}} \boldsymbol{M}^{-1})) = 0 \Leftrightarrow \\
&\quad \det(\lambda^2 \boldsymbol{I}^{\text{T}} + \lambda (\boldsymbol{M}^{-1}\boldsymbol{D})^{\text{T}} + \Omega_0 (\boldsymbol{J}^{\text{T}} \boldsymbol{M}^{-1})^{\text{T}}) = 0 \Leftrightarrow \\
&\quad \det(\lambda^2 \boldsymbol{I} + \lambda \boldsymbol{M}^{-1}\boldsymbol{D} + \Omega_0 (\boldsymbol{M}^{-1}\boldsymbol{J})) = 0
\end{aligned}
\tag{3}
$$

In the above derivation, the property $\det(\boldsymbol{X}^{\text{T}}) = \det(\boldsymbol{X})$ is used again, and $(\boldsymbol{M}^{-1}\boldsymbol{D})^{\text{T}} = \boldsymbol{M}^{-1}\boldsymbol{D}$ since $\boldsymbol{M}$ and $\boldsymbol{D}$ are both diagonal.

Apply eigen-decomposition for the third matrix term in (3), i.e., $\Omega_0 \boldsymbol{M}^{-1}\boldsymbol{J} = \boldsymbol{P} \boldsymbol{\Lambda} \boldsymbol{P}^{-1}$, $\boldsymbol{\Lambda} = \text{diag}(\mu_1, \mu_2, ..., \mu_n)$ and denote $\eta \boldsymbol{I} \approx \lambda^2 \boldsymbol{I} + \lambda \boldsymbol{M}^{-1}\boldsymbol{D}$. Then, (3) can be approximated by:

$$
\det(\eta \boldsymbol{I} + \boldsymbol{P} \boldsymbol{\Lambda} \boldsymbol{P}^{-1}) = \det(\eta \boldsymbol{P} \boldsymbol{P}^{-1} + \boldsymbol{P} \boldsymbol{\Lambda} \boldsymbol{P}^{-1}) = \det(\boldsymbol{P}(\eta \boldsymbol{I} + \boldsymbol{\Lambda}) \boldsymbol{P}^{-1}) = 0
\tag{4}
$$

Note that $\det(\boldsymbol{P}^{-1}) \cdot \det(\boldsymbol{P}) = \det(\boldsymbol{P}^{-1}\boldsymbol{P}) = \det(\boldsymbol{I}) = 1$ holds by the Laplace expansion theorem. Thus, (4) becomes:

$$
\det(\boldsymbol{P}) \cdot \det(\eta \boldsymbol{I} + \boldsymbol{\Lambda}) \cdot \det(\boldsymbol{P}^{-1}) = \det(\eta \boldsymbol{I} + \boldsymbol{\Lambda}) = 0
\tag{5}
$$

The final determinant in (5) leads to:

$$
\det \left(\begin{bmatrix} \eta_1 + \mu_1 & 0 & \cdots & 0 \\ 0 & \eta_2 + \mu_2 & \cdots & 0 \\ \vdots & \vdots & & \vdots \\ 0 & 0 & \cdots & \eta_n + \mu_n \end{bmatrix} \right) = \prod_{i=1}^{n} (\eta_i + \mu_i) = 0
\tag{6}
$$

Denote the system eigenvalues, i.e., oscillation modes, as $\lambda_i := \rho_i \pm j\omega_i \, (i = 1, 2, ..., n)$, where λ_i represents a pair of complex roots [1], [2]. Then, by solving a series of single-variable quadratic equations, i.e., $-\mu_i = \eta_i = \lambda_i^2 + (D_i/M_i)\lambda_i$, the analytical solution of the oscillation frequency can be obtained as:

$$
\left\{
\begin{aligned}
&-\mu_i = \lambda_i^2 + (D_i/M_i)\lambda_i \Rightarrow \lambda_i = \frac{-(D_i/M_i) \pm j \sqrt{4\mu_i - (D_i/M_i)^2}}{2} \\
&\lambda_i = \rho_i + j\omega_i \\
&\frac{1}{2\pi} \text{Im}(\lambda_i) = \frac{1}{4\pi} \sqrt{4\mu_i - (D_i/M_i)^2}
\end{aligned}
\right.
\tag{7}
$$

It can be verified that when all D_i are zeros, (7) will degenerate to an exact conclusion in Chapter 8 of [1] for that particular case.

III. UQ

In the UQ theory [11], [12], there are mainly two types of uncertainties: epistemic uncertainty (also known as systematic uncertainty, caused by limitations of human being's recognition or measurement ability, e.g., unknown-but-bounded parameters), and aleatory uncertainty (also known as stochastic uncertainty, caused by uncontrollable factors of probabilistic nature, e.g., climate change). In this paper, the former type is handled by interval analysis, e.g., treating f_i and D_i as unknown-but-bounded parameters. The latter type is handled by treating the interested variable as a random variate, e.g., f_i, depending on another random variable, e.g., D_i, whose probability distribution is given.

Note that, by (7), the proposed UQ method can also be adapted to study the uncertainty impacts of the system operating condition μ_i and generator inertia M_i, which is out of scope of this letter.

A. Interval Analysis

In (7), the condition $D_i^2 < 4M_i^2\mu_i$ (it can be verified that μ_i is real and nonnegative due to the near symmetricity of J and the positive diagonality of M) needs to be held to keep the argument of the square root positive; otherwise, λ_i is not an oscillation mode. Supposing $D_i \in [a,b] \supseteq [0, 2M_i\sqrt{\mu_i}]$ (in this letter, generator damping is considered nonnegative), the first- and second-order derivatives of f_i to D_i are:

$$
\begin{cases}
f_i' = \dfrac{-D_i}{4\pi M_i \sqrt{4\mu_i M_i^2 - D_i^2}} \\[2ex]
f_i'' = \dfrac{-\mu_i M_i}{\pi(4\mu_i M_i^2 - D_i^2)^{3/2}} \leq 0
\end{cases}
\tag{8}
$$

Thus, based on the signs of f_i' and the knowledge of calculus, the interval of f_i can be obtained as:

$$
f_i \in \left[f_i(b), \max\left\{ f_i(a), \frac{\sqrt{\mu_i}}{2\pi} \right\} \right]
\tag{9}
$$

B. Probabilistic Analysis

In (7), common distributions can be considered when treating D_i as random. For example, if it satisfies a normal distribution, i.e., $D_i \sim N(\zeta_i, \sigma_i^2)$, the cumulative distribution function (CDF) $F(x)$ of f_i can be derived as (10) based on (7).

$$
F(x) = P(f_i \leq x) = P(D_i^2 \geq 4M_i^2(\mu_i - 4\pi^2 x^2)) = P(|D_i| \geq d_i) =
$$

$$
1 - P(|D_i| \leq d_i) = 1 - \left(\Phi\left(\frac{d_i - \zeta_i}{\sigma_i}\right) - \Phi\left(\frac{d_i + \zeta_i}{-\sigma_i}\right) \right) =
$$

$$
2 - \Phi\left(\frac{d_i - \zeta_i}{\sigma_i}\right) - \Phi\left(\frac{d_i + \zeta_i}{\sigma_i}\right)
\tag{10}
$$

where $d_i := 2M_i\sqrt{|\mu_i - 4\pi^2 x^2|}$; and $\Phi(\cdot)$ is the CDF of the Gaussian distribution $N(0,1)$ (the standard normal distribution), which is readily available in most numerical computation software.

The expected value and variance of f_i can be computed by the following expressions based on the "delta method" in statistics theory [13], i.e., obtaining statistics by Taylor expansion:

$$
E(f_i(D_i)) \approx f_i(E(D_i)) + (Var(D_i)/2)f_i''(E(D_i))
\tag{11}
$$

$$
Var(f_i(D_i)) \approx (f_i'(E(D_i)))^2 Var(D_i)
\tag{12}
$$

where f_i, f_i', and f_i'' follow (7) and (8); and $E(\cdot)$ and $Var(\cdot)$ are the expectation and variance operators, e.g., $E(D_i) = \zeta_i$ and $Var(D_i) = \sigma_i^2$ when $D_i \sim N(\zeta_i, \sigma_i^2)$, respectively. Note that the above derivation process can be generalized to other common distributions based on (7).

IV. CASE STUDY I: IEEE 9-BUS SYSTEM

This section tests the proposed method on a modified IEEE 9-bus system [14], as shown in Fig. 2. The classic gen-

erator model is adopted here. The test includes two parts: the accuracy verification part for the derived estimation formula (7) and the UQ part based on (9) to (12). All the methods are implemented in MATLAB on a computer with a 4.0 GHz CPU and 16 GB RAM. Results for all the two oscillation modes are presented here. For the method acronyms, "*FULL*" means building the whole state-space matrix by directly linearizing the full-size DAEs of the original power system, i.e., without network reduction and considering all generator controllers if there exist, and then applying the MATLAB "eig" command, which provides a baseline result. "*SEP*" means using the "eig" command directly on the $2n$-by-$2n$ matrix A in (1). "*QEP*" means using (7), i.e., the proposed analytical formula in this letter.
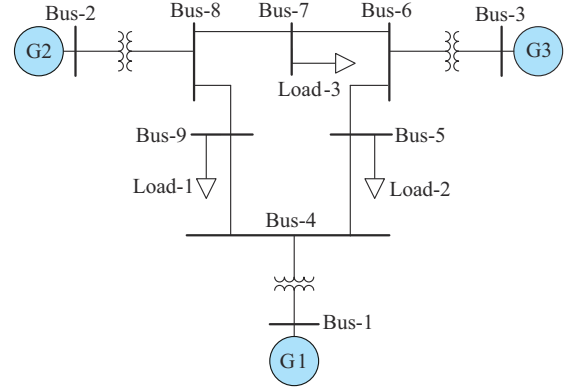

Fig. 2. IEEE 9-bus system topology.

A. Results of Frequency Estimation in IEEE 9-bus System

Comparison results for the base case scenario S_0, scenario-1 (load decreased by 5%, denoted as S_1), scenario-2 (load increased by 5%, denoted as S_2), scenario-3 (load decreased by 10%, denoted as S_3), and scenario-4 (load increased by 10%, denoted as S_4) are listed in Table I.

TABLE I
ESTIMATED OSCILLATION FREQUENCIES IN S_0 TO S_4 (IEEE 9-BUS SYSTEM)

Method	Scenario	f (Hz) Mode 1	Mode 2	Time (ms)
QEP	S_0	1.3825	2.1259	0.305
	S_1	1.3803	2.1248	0.271
	S_2	1.3843	2.1271	0.245
	S_3	1.3779	2.1237	0.281
	S_4	1.3858	2.1283	0.265
SEP	S_0	1.3825	2.1259	1.603
	S_1	1.3803	2.1248	1.373
	S_2	1.3843	2.1271	1.117
	S_3	1.3779	2.1237	1.142
	S_4	1.3858	2.1283	1.215
FULL	S_0	1.4006	2.1261	35.018
	S_1	1.3987	2.1254	31.931
	S_2	1.4021	2.1268	33.047
	S_3	1.3958	2.1242	31.588
	S_4	1.4025	2.1287	32.797

As observed, frequencies of all the oscillation modes obtained by the proposed method can match those by the *SEP* method and the *FULL* method in all three scenarios. The time cost of *FULL* method (already excluding the data reading time) is higher than the reduced network based the methods (*QEP*, *SEP*), but their frequency results are still close.

B. Results of UQ in IEEE 9-bus System

1) Results of Interval Analysis

Here, take the 2.1 Hz mode as an illustrative example. The dominant generator associated with that mode is the one at bus-3 based on (7). The base case D value of that generator is 3.01 p.u.. For the experiment of interval analysis, a set of 50 D values is drawn from an example interval [0, 6.02] for that generator. Then by (9), the lower and upper bounds for that mode can be analytically obtained as shown in Table II (denoted as f-LB and f-UB, respectively). The minimum and maximum values of all modes computed by the *SEP* method (over all the samples) are also listed.

TABLE II
RESULTS OF INTERVAL ANALYSIS (IEEE 9-BUS SYSTEM)

Mode No.	f-LB (analytical) (Hz)	f-UB (analytical) (Hz)	f_{min} (sampled) (Hz)	f_{max} (sampled) (Hz)
1	-	-	1.3824	1.3826
2	2.1248	2.1263	2.1249	2.1261

It can be observed that the sampled minimum and maximum values of that 2.1 Hz mode are within the analytically derived bounds, and the frequency of another oscillation mode is relatively less affected. The scatter plot is shown in Fig. 3(a), from which it can be observed that all sampled points are within the analytically derived bounds, which demonstrates the effectiveness of (9). One application of the above analytical bounds is that if a field-measured oscillation frequency is obviously outside of these bounds when other system conditions remain unchanged, it may be inferred that either the generator damping has abnormally varied or field measurements have been contaminated.
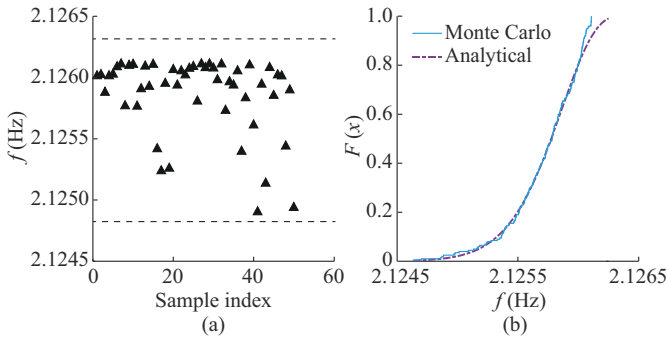

Fig. 3. UQ for 2.1 Hz mode in IEEE 9-bus system. (a) Interval analysis. (b) Probabilistic analysis.

2) Results of Probabilistic Analysis

Monte Carlo simulation setting: another set of 1000 values of D for the generator at bus-3 are sampled from an example normal distribution $N(\zeta = 3.01, \sigma^2 = 1.0)$. Then, eigen-

values are computed by the *SEP* method. Two CDF curves are shown in Fig. 3(b). As can be observed, the CDF by the analytically derived distribution in (10) can follow the trend of the CDF by the Monte Carlo simulation in a wide range.

The expected value by (11) and the standard deviation by (12) (as the square root) are listed in Table III. As observed, they can match the Monte Carlo statistics. The Monte Carlo method takes significantly more time due to its multi-run nature. One interpretation of the probabilistic result here is that: when other system conditions remain unchanged, the frequency of this oscillation mode is less volatile to the stochastic variation of the damping of generator-3 in this specific system.

TABLE III
RESULTS OF PROBABILISTIC ANALYSIS (IEEE 9-BUS SYSTEM)

Method	Expected value	Standard deviation	Time cost (ms)
Monte Carlo	2.1259	2.65×10^{-4}	64.7
Analytical (proposed)	2.1259	2.47×10^{-4}	1.1

V. CASE STUDY II: WECC 179-BUS SYSTEM

To demonstrate the effectiveness of the proposed method on complicated large power systems, a modified WECC system with 179 buses and 29 generators [15] is used in this section, as shown in Fig. 4. All its generators are represented by the 6th-order models plus governors and exciters in the original data. It represents the U.S. western power grid. The experimental settings are the same as in the previous case.

A. Results of Frequency Estimation in WECC 179-bus System

The results of two example modes are inspected here, of which one is a local mode with 1.71 Hz frequency (base case), and the other is an inter-area mode with 0.77 Hz frequency (base case). The meanings of the five scenarios (S_0-S_4) are the same as that described in Section IV. It can be observed in Table IV that the results of the proposed method (*QEP*) are again close to those of the other two methods in all three scenarios, which validates the accuracy of (7) on complicated large power systems.

B. Results of UQ in WECC 179-bus System

1) Results of Interval Analysis

Here, take the 1.71 Hz mode as an illustrative example. The dominant generator associated with that mode is the one at bus-6 based on (7). The value of base case D of that generator is 4.0 p.u.. A set of 50 D values are drawn from an example interval [0, 8.0] for that generator. Then by (9), the lower and upper bounds for that mode are presented in Table V. The minimum and maximum values of the two example oscillation modes computed by the *SEP* method (over all the samples) are also listed. It can be observed that the computed minimum and maximum values of 1.71 Hz mode are within its analytically derived bounds, and the frequency of the other mode is less affected. Similar conclusions can be drawn for the 0.77 Hz mode, and its results are omitted here. The scatter plot is shown in Fig. 5(a), where all the

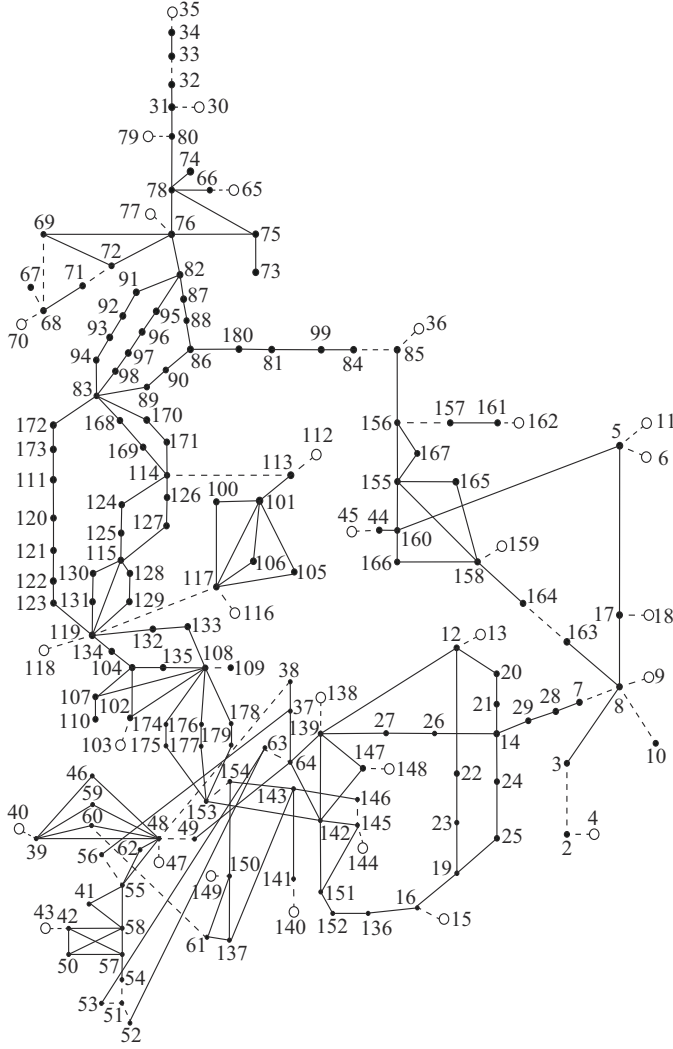samples are within the analytically derived bounds.

Fig. 4.   Topology of WECC 179-bus system.

TABLE IV
ESTIMATED OSCILLATION FREQUENCIES IN S_0 TO S_4
(WECC 179-BUS SYSTEM)

| Method | Scenario | f (Hz) | | Time (ms) |
		Mode 1	Mode 2	
QEP	S_0	1.7130	0.7740	0.997
	S_1	1.7222	0.7798	1.031
	S_2	1.7058	0.7748	1.065
	S_3	1.7101	0.6929	1.059
	S_4	1.7018	0.7534	0.988
SEP	S_0	1.7129	0.7736	8.964
	S_1	1.7221	0.7794	8.190
	S_2	1.7057	0.7735	7.981
	S_3	1.7100	0.6939	8.120
	S_4	1.7017	0.7529	8.062
FULL	S_0	1.7139	0.7745	70.727
	S_1	1.7181	0.7645	77.685
	S_2	1.7056	0.7726	75.374
	S_3	1.7199	0.7092	70.332

TABLE V
RESULTS OF INTERVAL ANALYSIS (WECC 179-BUS SYSTEM)

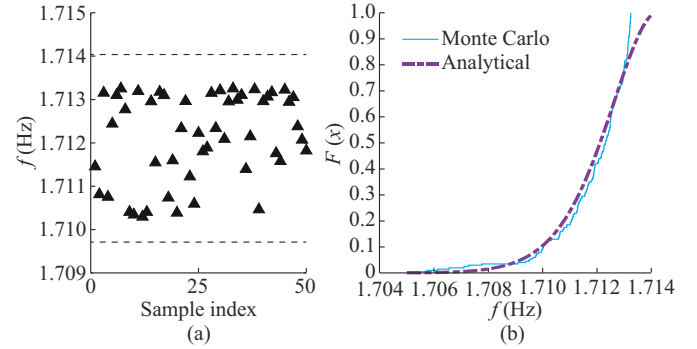| Mode No.	f-LB (analytical) (Hz)	f-UB (analytical) (Hz)	f_{min} (sampled) (Hz)	f_{max} (sampled) (Hz)
1	1.7097	1.714	1.7103	1.7133
2	-	-	0.7735	0.7737

Fig. 5.   UQ for 1.71 Hz mode in WECC 179-bus system. (a) Interval analysis. (b) Probabilistic analysis.

2) Results of Probabilistic Analysis

Monte Carlo simulation setting: another set of 1000 values of D for the generator at bus-5 are sampled from an example normal distribution $N(\zeta = 4.0, \sigma^2 = 3.6)$. Then eigenvalues are computed by the *SEP* method. Two CDF curves are shown in Fig. 5(b).

Again, the CDF curve by the analytically derived distribution in (10) can follow the trend of the CDF curve by the Monte Carlo simulation, and their statistics are close to each other, as shown in Table VI. As observed, the probabilistic variation of 1.71 Hz mode is around 0.0014 Hz, when the damping of generator-5 varies according to the above normal distribution in this specific system. Similar conclusions can be drawn for the 0.77 Hz mode, with its results omitted here.

TABLE VI
RESULTS OF PROBABILISTIC ANALYSIS (WECC 179-BUS SYSTEM)

Method name	Expected value	Standard deviation	Time cost (ms)
Monte Carlo	1.71186	0.00149	1346.8
Analytical (proposed)	1.71187	0.00138	1.8

VI.   CONCLUSION

An analytical UQ method for electromechanical oscillation frequencies is established regarding the impact of varying generator damping. When the uncertain intervals of the generator damping parameters are given, the uncertain intervals of the electromechanical oscillation frequencies can be analytically obtained. When typical probabilistic distributions, e.g., the normal distributions, of the generator damping coefficients are given, the analytical expressions of probabilistic distributions and statistics for the electromechanical oscillation frequencies can also be obtained. The accuracy and speed of the proposed method are demonstrated via com-

parison experiments. The next step is to combine the proposed analytical method with other numerical methods, e.g., AESOPS [16].

REFERENCES

[1] P. W. Sauer and M. A. Pai, *Power System Dynamics and Stability.* Upper Saddle River: Prentice Hall, 1998, pp. 249-253.

[2] P. Kundur, *Power System Stability and Control*. New York: McGraw Hill, 1994.

[3] F. Wang, L. Zhang, X. Feng *et al*., "An adaptive control strategy for virtual synchronous generator," *IEEE Transactions on Industrial Applications*, vol. 54, no. 5, pp. 5124-5133, Sept. 2018.

[4] A. Ademola-Idowu and B. Zhang, "Optimal design of virtual inertia and damping coefficients for virtual synchronous machines," in *Proceedings of 2018 IEEE PES General Meeting (PESGM)*, Portland, USA, Aug. 2018, pp. 1-5.

[5] L. Fan, "Interarea oscillations revisited," *IEEE Transactions on Power Systems*, vol. 32, no. 2, pp. 1585-1586, Mar. 2017.

[6] X. Bian, X. Huang, K. Wong *et al*., "Improvement on probabilistic small-signal stability of power system with large-scale wind farm integration," *International Journal of Electrical Power & Energy Systems*, vol. 61, pp. 482-488, Oct. 2014.

[7] Z. Yue, Y. Liu, Y. Yu *et al*., "Probabilistic transient stability assessment of power system considering wind power uncertainties and correlations," *International Journal of Electrical Power & Energy Systems*, vol. 117, p. 105649, May 2020.

[8] C. Xia, X. Zheng, L. Guan *et al*., "Probability analysis of steady-state voltage stability considering correlated stochastic variables," *International Journal of Electrical Power & Energy Systems*, vol. 131, p. 107105, May 2021.

[9] F. Tisseur and K. Meerbergen, "The quadratic eigenvalue problem," *SIAM Review*, vol. 43, no. 2, pp. 235-286, Aug. 2001.

[10] J. R. Silvester, "Determinants of block matrices," *Mathematical Gazette*, vol. 84, no. 501, pp. 460-467, Nov. 2000.

[11] H. G. Matthies, "Quantifying uncertainty: modern computational representation of probability and applications," in *Proceedings of NATO Advanced Research Workshop on Extreme Man-made and Natural Hazards in Dynamics of Structures*, Opatija, Croatia, May 2006, pp. 105-135.

[12] Wikipedia. (2023, Jan.). Uncertainty-quntification. [Online]. Available: https://en.wikipedia.org/wiki/Uncertainty_quantification

[13] J. L. Doob, "The limiting distributions of certain statistics," *The Annals of Mathematical Statistics*, vol. 6, no. 3, pp. 160-169, Jul. 1935.

[14] P. M. Anderson and A. A. Fouad, *Power System Control and Stability*. Piscataway: IEEE Press, 2003.

[15] S. Maslennikov. (2021, Aug.). Test cases library of power system sustained oscillations. [Online]. Available: http://web.eecs.utk.edu/~kaisun/Oscillation

[16] D. M. Lam, H. Yee, and B. Campbell, "An efficient improvement of the AESOPS algorithm for power system eigenvalue calculation," *IEEE Transactions on Power Systems*, vol. 9, no. 4, pp. 1880-1885, Jul. 1994.

Yongli Zhu received the B. S. degree in electrical engineering from Huazhong University of Science & Technology, Wuhan, China, in 2009, and the Ph. D. degree from the University of Tennessee, Knoxville, USA, in 2012. He has been working as a Postdoctoral Researcher at Texas A&M University, College Station, USA, since 2021. His research interests include power system reliability, stability, and artificial intelligence applications.

Chanan Singh is a University Distinguished Professor, Regents Professor, and Irma Runyon Chair Professor in the Department of Electrical and Computer Engineering, Texas A&M University, College Station, USA. He served as the Department Head of Electrical and Computer Engineering at Texas A&M University from 1997 to 2005 and then as an Interim Head from 2012 to 2015. He also served as a Program Director at the National Science Foundation of the USA and a Guest Professor at Tsinghua University, Beijing, China. He has authored/co-authored more than 400 technical papers and four books and has contributed to several books. He is a Member of the USA National Academy of Engineering and a Fellow of the Indian National Academy of Engineering. He is a Fellow of the IEEE and a Fellow of the Chinese Society of Electrical Engineering. He is the inaugural recipient of the IEEE-PES Roy Billinton Power System Reliability Award and the IEEE-PES Lifetime Achievement Award. His research interests include foundational developments and applications of probabilistic methods for planning and operation of electric power grid.